

# Dual-band terahertz antenna based on a novel photonic band gap structure\*

BAI Yukun and LI Jie\*\*

*Tianjin Key Laboratory of Film Electronic and Communication Devices, Engineering Research Center of Optoelectronic Devices and Communication Technology, Ministry of Education, School of Integrated Circuit Science and Engineering, Tianjin University of Technology, Tianjin 300384, China*

(Received 11 January 2023; Revised 20 February 2023)

©Tianjin University of Technology 2023

In this paper, a novel dual-band photonic band gap (PBG) structure was proposed and applied to a dual-band microstrip antenna. The antenna resonates at 1.267 THz and 1.502 THz, exhibiting reflection coefficients of  $-58.177$  dB and  $-49.462$  dB, and gains of 3.173 dBi and 5.232 dBi, respectively. Compared with the microstrip antenna based on the homogeneous silicon substrate, the designed dual-band antenna based on the novel PBG structure shows improved impedance matching, radiation efficiency, and gain. The paper simulated and analyzed the impacts of different filling dielectric materials and the variations of dimensions, position, period, and corrugation depths of the dual-band PBG structure on the resonances of the antenna. It is expected that the proposed novel dual-band PBG structure has great application potentials, and such cancer diagnosis is done by utilizing the radiation characteristics of the antenna.

**Document code:** A **Article ID:** 1673-1905(2023)11-0666-7

**DOI** <https://doi.org/10.1007/s11801-023-3005-1>

Applications of the terahertz band (0.1—10 THz) have evolved rapidly in the past decade because it constitutes the electromagnetic wave with the highest frequency in electronics and its single photon energy is merely one millionth of that of the X-ray. Besides, owing to its short wavelength, the terahertz wave can penetrate certain non-metallic or non-polar materials<sup>[1-5]</sup>. Moreover, the spectra of most macromolecules are in the terahertz band<sup>[6]</sup>. These bestow the terahertz wave with commendable characteristics, such as low damage<sup>[7]</sup>, high spectral resolution<sup>[8]</sup>, good visualization<sup>[9]</sup>, and broad bandwidth<sup>[10]</sup>, realizing extensive applications in the fields of biomedicine, sensing, and communications<sup>[11]</sup>. The terahertz antenna has also achieved rapid development owing to the advancement in 5G<sup>[12]</sup>, new materials<sup>[13]</sup>, and manufacturing technology<sup>[14]</sup>. In 2014, NEJATI et al<sup>[15]</sup> increased the gain and bandwidth of the patch antenna with a resonance frequency of 0.6 THz by loading a photonic band gap (PBG) structure on the polyimide substrate. In 2018, KUSHWAHA et al<sup>[16]</sup> optimized the terahertz patch antenna with a PBG structure loaded on a polyimide substrate, achieving a gain of 7.934 dBi at a resonance frequency of 0.630 8 THz. In 2019, VAHDATI et al<sup>[17]</sup> introduced the design of a high-frequency patch antenna with a resonance frequency of 1.4 THz by loading a PBG structure on the Rogers5880 substrate. In 2021, THAKUR et al<sup>[18]</sup> used a

0.198 THz patch antenna with a PBG structure loaded on a polyimide substrate for cancer detection.

Currently, the resonance frequency of designed terahertz patch antennas is between 0.1 THz and 1 THz<sup>[2]</sup>, and the proposed PBG structure only applies to a single resonance frequency.

In this paper, a new dual-band PBG structure is designed and applied to a dual-band microstrip antenna with resonance frequencies of 1—2 THz, significantly improving the antenna performance. The design bases of the PBG structure and dual-band antenna are discussed. The influence of the dielectric material filled in the dual-band PBG structure on the antenna performance is simulated. The influence of geometric parameters of the dual-band PBG structure on the antenna resonances is discussed.

The design of the dual-band PBG structure and dual-band circular microstrip antenna, as shown in Fig.1, is introduced in this section.

The antenna substrate is made of silicon, for which the dielectric constant is 11.9, and the loss tangent is 0.000 25. The dual-band PBG structure comprises a two-dimensional periodic ring cavity array corrugated in the upper part of the substrate (upper cavity array) and a two-dimensional periodic ring cavity array corrugated in the lower part of the substrate (lower cavity array), which are filled with dielectric materials (refer to

\* This work has been supported in part by the Natural Science Foundation of Tianjin (No.19JCYBJC16100), and in part by the Tianjin Innovation and Entrepreneurship Training Program (No.202210060027).

\*\* E-mail: li1336014116@163.com

Fig.1(b)—(d)). In this way, PBG provides resistance to surface waves propagating inside the substrate, achieving improved gain, directionality, bandwidth, and radiation<sup>[19]</sup>.

The dielectric constant varies periodically on PBG and is denoted by  $\varepsilon(r)$ , where  $r$  is the position vector of PBG. The angular frequency is  $\omega$ , and the PBG equation corresponding to the polarization of  $E$  and  $H$  is<sup>[20]</sup>

$$\frac{1}{\varepsilon(r)} \left( \frac{\partial^2}{\partial x^2} + \frac{\partial^2}{\partial y^2} \right) E_z(r) + \frac{\omega^2}{c^2} E_z(r) = 0,$$

$$\frac{\partial}{\partial x} \left[ \frac{1}{\varepsilon(r)} \frac{\partial H_z}{\partial x} \right] + \frac{\partial}{\partial y} \left[ \frac{1}{\varepsilon(r)} \frac{\partial H_z}{\partial y} \right] + \frac{\omega^2}{c^2} H_z(r) = 0. \quad (1)$$

According to the above analysis, the electromagnetic wave incident on the PBG will be decomposed into  $E$ -polarization and  $H$ -polarization, which correspond to different equations.

A single-band circular patch antenna is designed based on the microstrip antenna theory, as demonstrated in Fig.1(a). The working frequency  $f_r$ , the relative dielectric constant  $\varepsilon_r$ , and the height  $h$  ( $\mu\text{m}$ ) of the substrate are pre-determined. The effective radius of the circular patch antenna can be computed from its geometric radius  $R_a$  using the following formula<sup>[21]</sup>

$$R = (2M + 1) \times R_a \left\{ 1 + \frac{2h}{\pi R_a \varepsilon_r} \left[ \ln \left( \frac{\pi R_a}{2h} \right) + 1.7726 \right] \right\}^{1/2}, \quad (2)$$

where

$$R_a = \frac{F}{\left\{ 1 + \frac{2h}{\pi \varepsilon_r F} \left[ \ln \left( \frac{\pi F}{2h} \right) + 1.7726 \right] \right\}^{1/2}},$$

$$F = \frac{8.791 \times 10^9}{f_r \sqrt{\varepsilon_r}}, \quad (3)$$

where  $M$  is a non-negative integer (in the present work,  $M=1$ ). Using the above expression and assuming that the antenna resonates at 1.267 THz, the following expression can be used to calculate the upper limit of the substrate thickness  $h$

$$h = \frac{\lambda_0}{4 \times \sqrt{\varepsilon_r}}, \quad (4)$$

and actual height is  $h=20 \mu\text{m}$ . The width ( $W_f$ ) of the feedline can be determined as follows

$$W_f = \frac{11.96 \lambda_0}{Z_a}, \quad (5)$$

where  $Z_a$  indicates the normalized impedance of the antenna, and  $\lambda_0$  represents the free space wavelength.

As illustrated in Fig.1, a rectangular slot with length  $S$  and width  $T$  is introduced on the circular patch of the single-band antenna, and the dual-band PBG structure is loaded on the substrate. This forms a dual-band patch antenna based on the dual-band PBG structure. Based on the above design, a circular patch is used on the top of the PBG substrate to excite resonance in the THz frequency region and then the antenna was driven along the

microstrip, and the antenna structure is designed with the geometrical parameters specified in Tab.1.

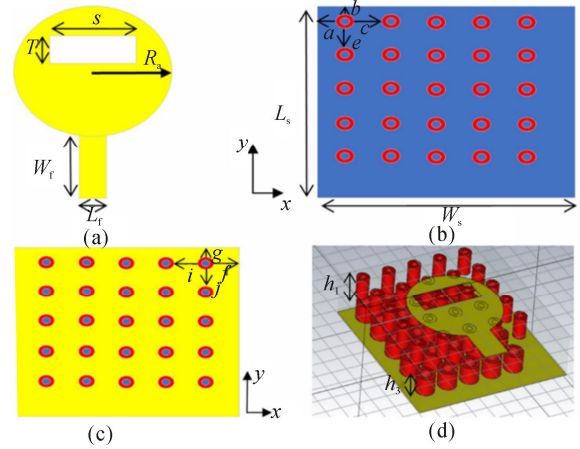


**Fig.1 Dual-band patch antenna based on the dual-band PBG structure: (a) Radiating patch; (b) Upper cavity array (radiating patch); (c) Lower cavity array; (d) Inside view of the designed dual-band PBG structure**

**Tab.1 Geometrical parameters of the designed antenna**

Parameter	Value ( $\mu\text{m}$ )	Parameter	Value ( $\mu\text{m}$ )
$W_f$	15.6	$e$	8.5
$g$	4	$L_f$	20.6
$W_s$	100	$L_s$	100
$i$	3	$R_a$	28.9
$j$	6	$a$	8
$S$	39	$T$	15
$b$	3	$c$	9.5
$R_1$	4	$R_2$	2
$R_3$	6	$R_4$	3.5
$h_1$	10	$h_3$	8
$f$	7.5		

CST Microwave Studio is used to design the antenna. The antenna performance is analyzed from the perspectives of reflection coefficient, gain, and standing wave ratio. Based on the uniform silicon substrate, the influence of the dielectric material filled in the PBG structure on the radiation characteristics of the antenna is discussed in this section, which includes the upper cavity array and the lower cavity array. The five types of antenna are defined as follows.

Type A: This type of antenna is based on a uniform silicon substrate and is devoid of the PBG structure.

Type B: The PBG structure is loaded, and the upper and lower cavities are filled with gallium arsenide (relative dielectric constant is  $\varepsilon_r=12.9$ ).

Type C: The PBG structure is loaded, the upper cavity is filled with polyimide (relative dielectric constant is  $\varepsilon_r=3.5$ ), and the lower cavity is filled with gallium arsenide.

Type D: The PBG structure is loaded, the upper cavity is filled with gallium arsenide, and the lower cavity is filled with polyimide.

Type E: The PBG structure is loaded, and both cavity arrays are filled with polyimide.

The detailed geometric parameters of the five antennas are enlisted in Tab.1. Type A antenna is a terahertz antenna based on a uniform substrate, which is used as a reference to evaluate the performance of the other types of antennas. Type B, C, D and E antennas are terahertz antennas which are loaded with ring cavities filled with different materials. It can be observed from Fig.2 that the antennas loaded with the PBG structure exhibit better performance in reflection coefficient, gain, and standing wave ratio compared with the reference Type A. Among the antennas loaded with the PBG structure, Type E illustrates the best reflection coefficient, gain, and standing wave ratio. One resonance frequency is at 1.267 THz (relative bandwidth of 1.7%), the reflection coefficient is reduced to  $-58.177$  dB, the standing wave ratio is 1.002 8, the radiation efficiency is 86.4%, and the gain is 3.173 dBi. The other resonance frequency is at 1.502 THz (relative bandwidth of 3.0%), the reflection coefficient is reduced to  $-49.762$  dB, the standing wave ratio is 1.006 6, the radiation efficiency is 89.2%, and the gain is 5.232 dBi. When the periodic variation in the dielectric constant of the two different materials is sufficiently large, the dispersion relationship of the electromagnetic wave propagating in it becomes very different from the original, leading to a band gap (i.e., PBG structure) where the electromagnetic wave cannot propagate<sup>[22]</sup>. Furthermore, the Type E PBG antenna with the largest dielectric constant difference (the difference between the dielectric constants of polyimide and silicon) is better than Type B, C and D antennas. Therefore, Fig.2 reveals that the PBG structure can effectively eliminate the surface wave effect of the antenna, and the larger the difference in the dielectric constant of the PBG structure, the more obvious the effect on the antenna.

The PBG substrate has a periodic ring cavity, whose geometric parameters can alter the resonances of the antenna. For the  $50 \Omega$  feed port setting, the influence of the geometric parameters of the ring cavity on the antenna resonance frequencies is simulated and analyzed in this section. The geometric parameters discussed in this section include the cavity's radius, period, filling depth, and position. Refer to Tab.1 for design parameters.

In the case of a dual-band antenna loaded with the PBG structure, the outer radius  $R_1$  of the upper cavity is increased from  $3 \mu\text{m}$  to  $5 \mu\text{m}$  with a step of  $1 \mu\text{m}$ , whereas the inner radius  $R_2$  is increased from  $1 \mu\text{m}$  to  $3 \mu\text{m}$  with a step of  $1 \mu\text{m}$ . Similarly, the outer radius  $R_3$  and the inner radius  $R_4$  of the lower cavity are increased from  $5 \mu\text{m}$  to  $7 \mu\text{m}$  and from  $2.5 \mu\text{m}$  to  $4.5 \mu\text{m}$  with steps of  $1 \mu\text{m}$ , respectively. As demonstrated in Fig.3, for the PBG ring cavity, the antenna resonance frequency increases with the increase in  $R_1$  and  $R_3$  and decreases

with the increase in  $R_2$  and  $R_4$ . Since the PBG structure is built by loading a polyimide-filled ring cavity on a uniform silicon substrate, the structure of the PBG substrate alters when the radius of the ring cavity is modified. Therefore, its effective dielectric constant changes, leading to the shift of the resonance frequency. The simulation results in Fig.3 also illustrate that when other radii of the cavities are fixed as in Tab.1, the individual setting of  $R_1=4 \mu\text{m}$ ,  $R_2=2 \mu\text{m}$ ,  $R_3=6 \mu\text{m}$ , and  $R_4=3.5 \mu\text{m}$  leads to the smallest reflection of the antenna, and an optimum matching effect between feed line and antenna is achieved.

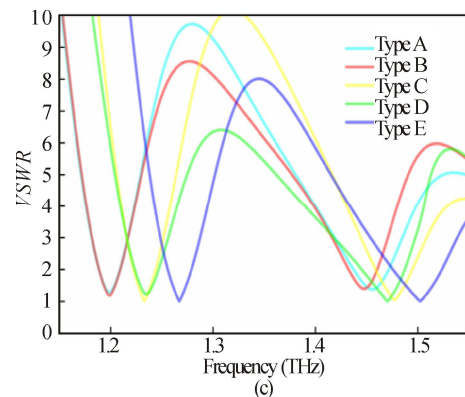
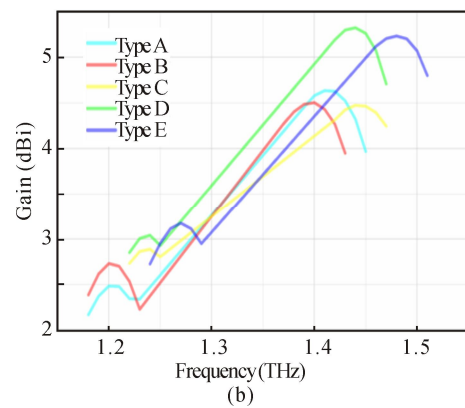
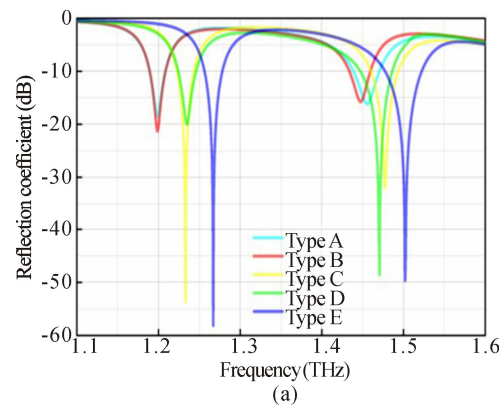
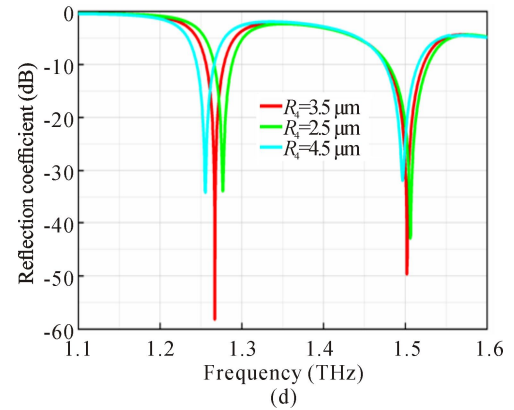
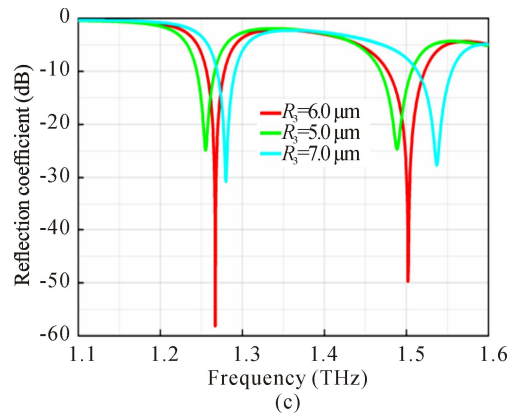


**Fig.2 Comparison among antennas based on a homogeneous silicon substrate and PBG substrates filled with different dielectric materials: (a) Reflection coefficient; (b) Gain; (c) VSWR**

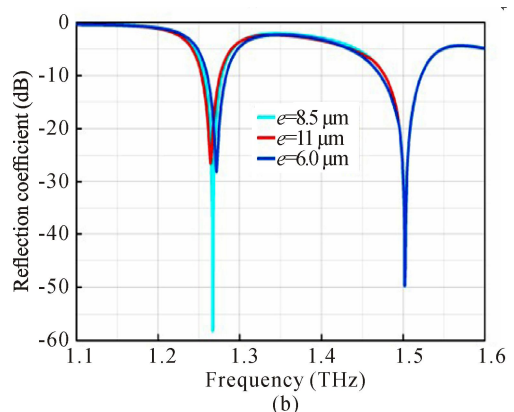
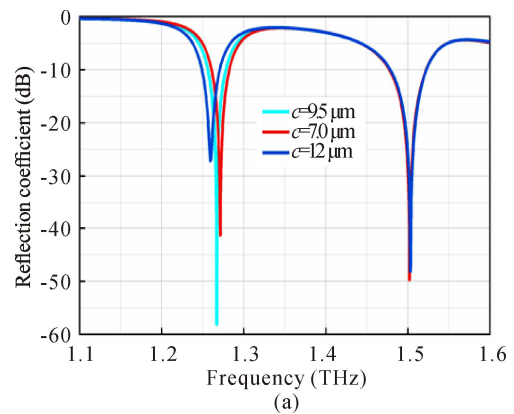
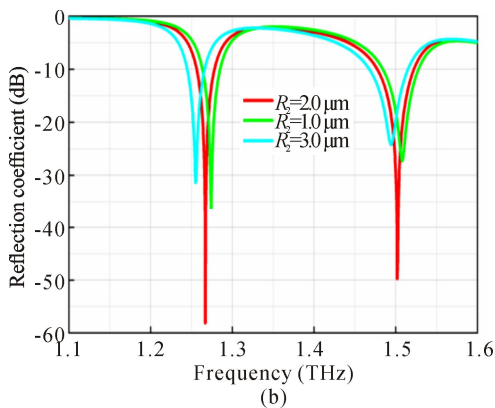
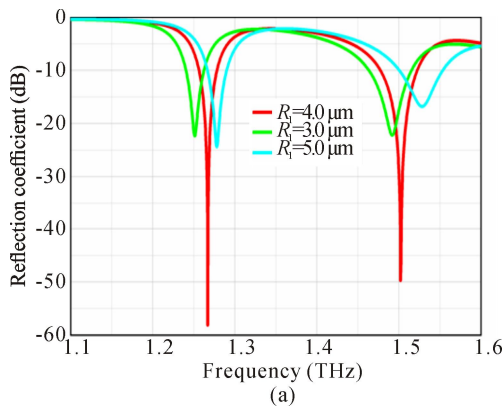
In 2015, NEJATI *et al.*<sup>[15]</sup> proved that the arrangement and shape of photonic crystals are the key parameters affecting the material properties, such as effective dielectric constant, magnetic permeability, and negative reflection. The results in Fig.3 also infer that the resonance frequency changes with the radius of the ring cavity in the PBG structure. This suggests that in addition to the arrangement and shape, the size of the PBG structure also causes changes in the effective dielectric constant and permeability of the photonic crystal, leading to certain changes in the resonance frequency of the antenna.

In the *x*-axis direction, the distance *c* between the upper cavities is increased from 7 μm to 12 μm with a step of 2.5 μm, whereas the distance *i* between the lower cavities is increased from 1 μm to 5 μm with a step of 2 μm. In the *y*-axis direction, the distance *e* between the upper cavities is increased from 6 μm to 11 μm with a step of 2.5 μm, whereas the distance *j* between the lower cavities is increased from 4 μm to 8 μm with a step of 2 μm (refer to Fig.1(b) and (c)).

The simulation results in Fig.4(a) and (b) reveal that for the PBG ring cavity, the first resonance frequency of the dual-band antenna reduces with the increase of *c* and *e*, i.e., the period of the upper cavity. Fig.4(c) and (d) reveals that the second resonance frequency of the dual-band antenna decreases with the increase of *i* and *j*, i.e., the period of the lower cavity. Meanwhile, it can be inferred from the simulation results of Fig.4 that when the other periods are unchanged, individual setting of *c*=9.5 μm, *e*=8.5 μm, *i*=3 μm, and *j*=6 μm leads to the smallest reflection of the antenna, and the matching effect between the feed line and antenna is optimized.



**Fig.3 Influence of the radius variation of the PBG ring cavities on the reflection coefficient: (a) Outer radius of the upper cavity; (b) Inner radius of the upper cavity; (c) Outer radius of the lower cavity; (d) Inner radius of the lower cavity**



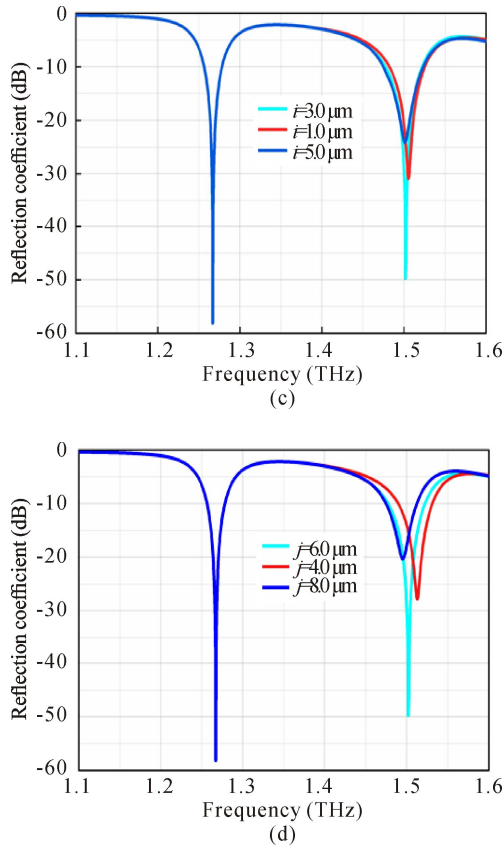
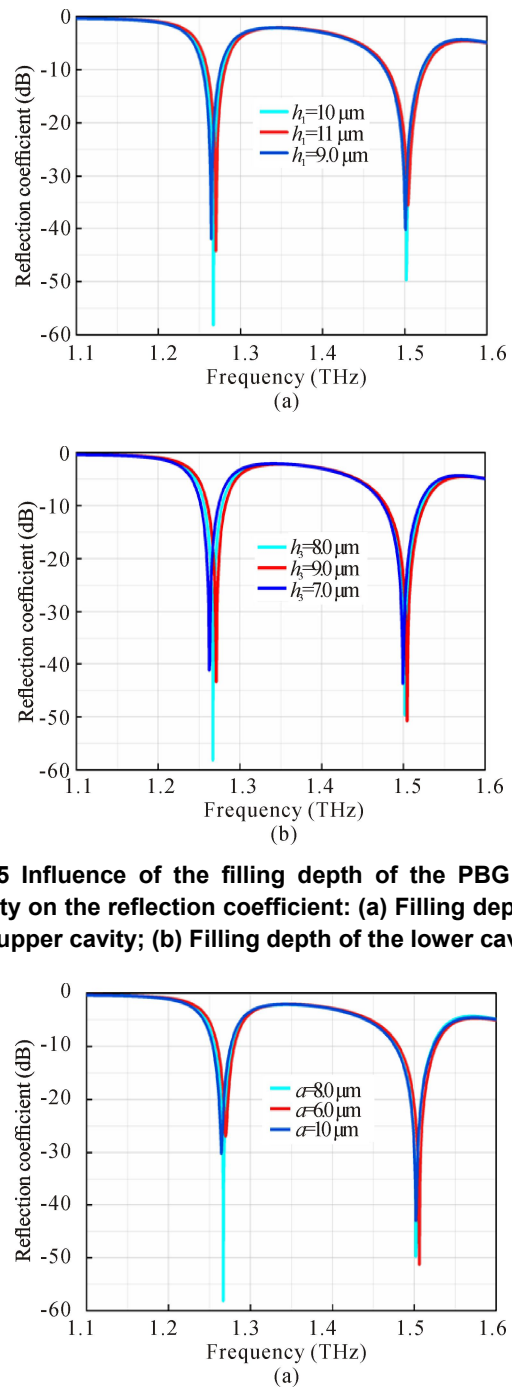


**Fig.4 Influence of the period variation of the PBG ring cavities on the reflection coefficient: (a) Period of the upper cavity in the x direction; (b) Period of the upper cavity in the y direction; (c) Period of the lower cavity in the x direction; (d) Period of the lower cavity in the y direction**

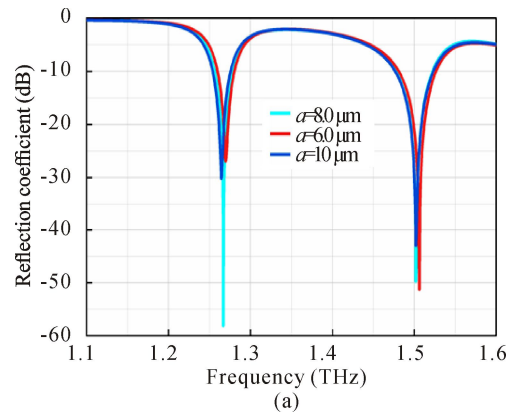
The filling depth  $h_1$  of the upper cavity is increased from  $9\ \mu\text{m}$  to  $11\ \mu\text{m}$ , whereas the filling depth  $h_3$  of the lower cavity is increased from  $7\ \mu\text{m}$  to  $9\ \mu\text{m}$ , both with a step of  $1\ \mu\text{m}$  (refer to Fig.1(d)). As represented in Fig.5, for the ring cavity with the PBG structure, the resonance frequency of the dual-band antenna increases with the increase of  $h_1$  and  $h_3$ . The change in filling depth alters the effective dielectric constant, leading to the frequency shift. The simulation results in Fig.5 also demonstrate that when the depth of the other ring cavity array is fixed as in Tab.1, individual setting of  $h_1=10\ \mu\text{m}$  and  $h_3=8\ \mu\text{m}$  leads to the smallest reflection of the antenna, and the matching effect between the feed line and antenna is the best.

In the  $x$ -axis direction, the distance  $a$  between the upper cavity and substrate edge is increased from  $6\ \mu\text{m}$  to  $10\ \mu\text{m}$ , with a step of  $2\ \mu\text{m}$ , whereas the distance  $f$  between the lower cavity and substrate edge is increased from  $5\ \mu\text{m}$  to  $10\ \mu\text{m}$ , with a step of  $2.5\ \mu\text{m}$ . In the  $y$ -axis direction, the distance  $b$  between the upper cavity and substrate edge is increased from  $1\ \mu\text{m}$  to  $5\ \mu\text{m}$ , with a step of  $2\ \mu\text{m}$ , whereas the distance  $g$  between the lower cavity and substrate edge is increased from  $2.5\ \mu\text{m}$  to  $5.5\ \mu\text{m}$ , with a step of  $1.5\ \mu\text{m}$  (refer to Fig.1(b) and (c)).

As illustrated in Fig.6, with the change of  $a$ ,  $b$ ,  $f$  and  $g$ , i.e., the position of the ring cavity on the substrate, the resonance frequency barely changes, but the reflection coefficient increases. This suggests that changing the position of the ring cavity has a significant impact on the impedance matching to the feed line. The reflection coefficient of the antenna input port increases as the position deviates from the matching position. The simulation results in Fig.6 also reveal that when the other position parameters are fixed as in Tab.1, individual setting of  $a=9.5\ \mu\text{m}$ ,  $b=3\ \mu\text{m}$ ,  $f=7.5\ \mu\text{m}$ , and  $g=4\ \mu\text{m}$  leads to the smallest reflection, and the matching effect between the feed line and the antenna is optimized.



**Fig.5 Influence of the filling depth of the PBG ring cavity on the reflection coefficient: (a) Filling depth of the upper cavity; (b) Filling depth of the lower cavity**



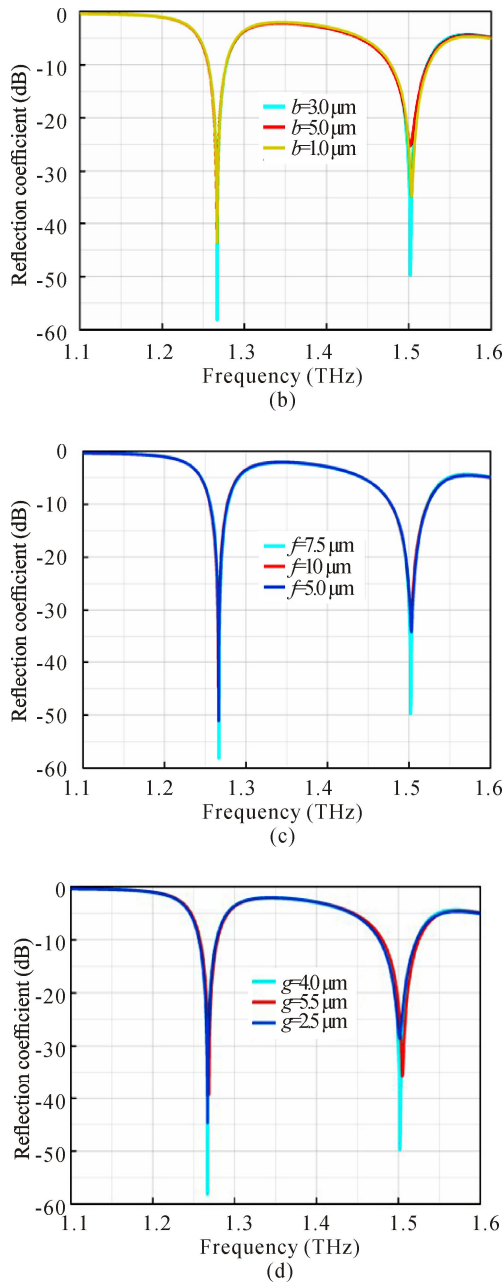


**Fig.6 Influence of the position of the PBG ring cavity on the reflection coefficient: (a) Distance between the upper cavity and the substrate edge in the x direction; (b) Distance between the upper cavity and the substrate edge in the y direction; (c) Distance between the lower cavity and the substrate edge in the x direction; (d) Distance between the lower cavity and the substrate edge in the y direction**

In this paper, the dual-band antenna operating at 1.267 THz and 1.502 THz and having a PBG structure substrate filled with different dielectric materials are designed and compared with the antenna based on a uniform silicon substrate. The simulation results reveal that the Type E antenna with polyimide filled in both the upper and lower cavity arrays exhibits the optimum reflection coefficient, standing wave ratio, and gain (refer to Fig.2). The influence of the geometric parameters of the

dual-band PBG structure on the antenna resonances is also investigated. The designed dual-band terahertz antenna is compared with the existing terahertz antenna with a PBG structure, as mentioned in Tab.2.

**Tab.2 Comparison of the designed PBG antenna with the existing PBG antennas**

Reference	Dual-band	Frequency (THz)	S11 (dB)	VSWR	Gain (dBi)
[15]	No	0.67	-24	—	5.52
[16]	No	0.630 8	-44.71	1.011 5	7.934
[23]	No	0.888 2	-56.573 4	1.002 8	—
[18]	Yes	0.198, 0.319	-68.53, -32.72	1.000 7, 1.04	3.43, —
[24]	No	0.63	-59.15	1.001	9.45
This work	Yes	1.267, 1.50	-58.18, -49.76	1.002, 1.006	3.17, 5.23

The comparison highlights that the designed dual-band antenna functions well at both resonance frequencies, demonstrating the prospects of the proposed dual-band PBG structure to be applied to various dual-band terahertz antennas, and it could be used for the early detection of cancer<sup>[25]</sup>.

**Ethics declarations**

**Conflicts of interest**

The authors declare no conflict of interest.

**References**

- [1] SWATHI P, ANJUM N N. Design of microstrip patch antenna for 2.45 GHz wireless applications[J]. Journal of recent research in engineering and technology, 2015, 2(4).
- [2] HE Y, CHEN Y, ZHANG L, et al. An overview of terahertz antennas[J]. China communications, 2020, 17(7): 124-165.
- [3] GEETHARAMANI G, AATHMANESAN T. Split ring resonator inspired THz antenna for breast cancer detection[J]. Optics & laser technology, 2020, 126: 106111.
- [4] DASH S, PATNAIK A. Impact of silicon-based substrates on graphene THz antenna[J]. Physica E : low-dimensional systems and nanostructures, 2021, 126: 114479.
- [5] SACHAN R, DHUBKARYA D C. Photonic band gap structure microstrip patch antenna for WiMAX and Wi-Fi application[J]. Photonic network communications, 2021, 41(3): 280-286.
- [6] DAS S, MITRA D, CHAUDHURI S R B. Fractal loaded circular patch antenna for super wide band operation in THz frequency region[J]. Optik, 2021, 226: 165528.
- [7] PEREIRA J P P, DA SILVA J P, DE Á, et al. Microstrip antennas design based in periodic and quasiperiodic PBG symmetries[J]. Microwave and optical technology

- letters, 2015, 57(12): 2914-2917.
- [8] PEREIRA J P P, DA SILVA J P, DE ANDRADE H D. A new design and analysis of a hexagonal PBG microstrip antenna[J]. Microwave and optical technology letters, 2015, 57(9): 2147-2151.
- [9] DA SILVA J L, DE ANDRADE H D, MAIA A S, et al. Performance of microstrip patch antenna due EBG/PBG arrangements insertion[J]. Microwave and optical technology letters, 2016, 58(12): 2933-2937.
- [10] SAMINENI P, KHAN T, DE A. Modeling of electromagnetic band gap structures: a review[J]. International journal of RF and microwave computer - aided engineering, 2017, 27(2): e21055.
- [11] KUSHWAHA R K, KARUPPANAN P, SRIVASTAVA Y. Proximity feed multiband patch antenna array with SRR and PBG for THz applications[J]. Optik, 2018, 175: 78-86.
- [12] KHEZZAR D, KHEDROUCHE D, DENIDNI T A. New design of a broadband PBG-based antenna for THz band applications[J]. Photonics and nanostructures-fundamentals and applications, 2021, 46: 100947.
- [13] JHA K R, SINGH G. Analysis and design of terahertz microstrip antenna on photonic bandgap material[J]. Journal of computational electronics, 2012, 11(4): 364-373.
- [14] KAZEMI F. Dual band compact fractal THz antenna based on CRLH-TL and graphene loads[J]. Optik, 2020, 206: 164369.
- [15] NEJATI A, SADEGHZADEH R A, GERAN F. Effect of photonic crystal and frequency selective surface implementation on gain enhancement in the microstrip patch antenna at terahertz frequency[J]. Physica B: condensed matter, 2014, 449: 113-120.
- [16] KUSHWAHA R K, KARUPPANAN P, MALVIYA L D. Design and analysis of novel microstrip patch antenna on photonic crystal in THz[J]. Physica B: condensed matter, 2018, 545: 107-112.
- [17] VAHDATI A, PARANDIN F. Antenna patch design using a photonic crystal substrate at a frequency of 1.6 THz[J]. Wireless personal communications, 2019, 109(4): 2213-2219.
- [18] THAKUR S, SINGH N. Circular-slot THz antenna on PBG substrate for cancer detection[J]. Optik, 2021, 242: 167355.
- [19] WANG Y. Design of microstrip antenna based on left-hand materials and photonic bandgap structure[D]. Xian: University of Electronic Science and Technology of Xian, 2015: 20-36. (in Chinese)
- [20] CHEN C. Calculation of band structure of two-dimensional photonic crystal[D]. Lanzhou: Lanzhou University, 2009: 3-7. (in Chinese)
- [21] RABBANI M S, GHAFOURI-SHIRAZ H. Size improvement of rectangular microstrip patch antenna at MM-wave and terahertz frequencies[J]. Microwave and optical technology letters, 2015, 57(11): 2585-2589.
- [22] NEJATI A, ZARRABI F B, RAHIMI M, et al. The effect of photonic crystal arrangement on metamaterial characteristic at THz domain[J]. Optik-international journal for light and electron optics, 2015, 126(19): 2153-2156.
- [23] KUSHWAHA R K, KARUPPANAN P. Enhanced radiation characteristics of graphene-based patch antenna array employing photonic crystals and dielectric grating for THz applications[J]. Optik, 2020, 200: 163422.
- [24] AHMAD I, ULLAH S, ULLAH S, et al. Design and analysis of a photonic crystal based planar antenna for THz applications[J]. Electronics, 2021, 10(16): 1941.
- [25] SHI J, TIAN L L, SU M Y, et al. Based on the surface of the terahertz optical fiber Bragg biosensor[J]. Journal of optoelectronics-lasers, 2022, 33(2): 127-132. (in Chinese)